Brevicidine, a bacterial non-ribosomally produced cyclic antimicrobial lipopeptide with a unique *modus operandi*

Xinghong Zhao[a,b,c,1,*], Xinyi Zhong[a,1], Hongping Wan[c,1], Lu Liu[a], Xu Song[a], Yuanfeng Zou[a], Lixia Li[a], Renyong Jia[c], Juchun Lin[a], Huaqiao Tang[a], Shan Zhao[c], Yifei Lang[c], Zhongqiong Yin[a,*], Oscar P. Kuipers[b]

[a] Centre for Sustainble Antimicrobials, Department of Pharmacy, Sichuan Agricultural University, Chengdu, 611130, China.

[b] Department of Molecular Genetics, Groningen Biomolecular Sciences and Biotechnology Institute, University of Groningen, Groningen, 9747 AG, The Netherlands.

[c] Key Laboratory of Animal Disease and Human Health of Sichuan Province, Sichuan Agricultural University, Chengdu, 611130, China.

[1] These authors contributed equally to this work.

* Correspondence: xinghong.zhao@sicau.edu.cn; yinzhongq@163.com

Abstract

Due to the accelerated appearance of antibiotic-resistant (AMR) pathogens in clinical infections, new first-in-class antibiotics, operating via novel modes of action, are desperately-needed. Brevicidine, a bacterial non-ribosomally produced cyclic lipopeptide, has shown potent and selective antimicrobial activity against Gram-negative pathogens. However, before our investigations, little was known about how brevicidine exerts its potent bactericidal effect against Gram-negative pathogens. In this study, we find that brevicidine has potent antimicrobial activity against AMR *Enterobacteriaceae* pathogens, with a MIC value ranging between 0.5μM and 2μM. In addition, brevicidine showed potent anti-biofilm activity against the *Enterobacteriaceae* pathogens, with same 100% inhibition and 100% eradication concentration of 4μM. Further mechanistic studies showed that brevicidine exerts its potent bactericidal activity via interacting with lipopolysaccharide in the outer membrane, targeting phosphatidylglycerol and cardiolipin in the inner membrane, and dissipating the proton motive force of bacteria. This results in metabolic perturbation, including inhibition of adenosine triphosphate synthesis, inhibits the dehydrogenation of nicotinamide adenine dinucleotides, accumulation of reactive oxygen species in bacteria, and inhibition of protein synthesis. Lastly, brevicidine showed a good therapeutic effect in a mouse peritonitis–sepsis model. Our findings pave the way for further research on clinical applications of brevicidine, to combat the prevalent infections caused by AMR Gram-negative pathogens worldwide.

Keywords: Brevicidine; Antimicrobial resistance; Antimicrobial mechanism; Bacteraemia model; *Escherichia coli*

Author summary

Due to the accelerated appearance of antimicrobial resistance in bacterial pathogens, many bacterial infections have become increasingly difficult, or even impossible, to treat with conventional antimicrobials. To address the problem posed by drug-resistant infections new first-in-class antibiotics, operating via novel modes of action, are desperately needed. Here, we show that the bacterial non-ribosomally produced cyclic antimicrobial lipopeptide brevicidine has potent antimicrobial against multi-drug resistance Gram-negative pathogens, with a MIC value ranging between 0.5μM and 2μM. Mechanism studies elucidate that brevicidine exerts its potent bactericidal activity via interacting with lipopolysaccharide in the outer membrane, targeting phosphatidylglycerol and cardiolipin in the inner membrane, and dissipating the proton motive force of bacteria. In addition, brevicidine showed a good therapeutic effect in a mouse peritonitis–sepsis model. This study showcases the excellent antibiotic properties of brevicidine in an age where new antibiotics that target Gram-negative bacteria are desperately needed.

57 ## Introduction

58 Due to the accelerated appearance of antimicrobial resistance (AMR) in bacterial
59 pathogens, many bacterial infections have become increasingly difficult, or even
60 impossible, to treat with conventional antimicrobials. The O'Neill report on AMR,
61 published in 2014, predicted that deaths attributable to resistant infections will reach
62 10 million annually by 2050 [1,2]. In addition, due to the COVID-19 pandemic, the
63 AMR situation is getting worse since increasing evidence has emerged that the
64 COVID-19 pandemic also contributes to AMR [2–6]. Despite the AMR situation being
65 so urgent, the number of newly approved antimicrobials has been steadily decreasing
66 over the past 20 years, especially those for treating Gram-negative pathogen
67 infections [7–9]. Bacteria produce a wealth of non-ribosomally produced peptide
68 (NRP) antimicrobials, including clinically approved antimicrobial cyclic lipopeptides,
69 such as vancomycin, daptomycin, and colistin [10]. This shows that the group of cyclic
70 lipopeptides makes up a rich source of molecules able to control pathogenic bacterial
71 infections.

72 Brevicidine (Bre), a bacterial non-ribosomally produced cyclic lipopeptide, was first
73 isolated from the *Brevibacillus laterosporus* DSM25 in 2018 [11]. This cyclic
74 lipopeptide contains 12 amino acids (4-Methyl-Hexanoyl-D-Asn-D-Tyr-D-Trp-D-Orn-
75 Orn-Gly-D-Orn-Trp-Thr-Ile-Gly-Ser) with a 4-Methyl-Hexanoyl chain at its N-terminus
76 and a lactone bond between Thr9 and Ser12 (Fig 1) [11,12]. Brevicidine displays
77 potent and selective antimicrobial activity against Gram-negative pathogens,
78 including *Enterobacter cloacae*, *Escherichia coli*, *Pseudomonas aeruginosa*, and
79 *Klebsiella pneumoniae* [11], which are listed as "critical" priority pathogens that need

R&D of new antimicrobials by the World Health Organization (WHO) [13]. Notably, brevicidine showed no cytotoxicity and hemolytic activity at a relatively high concentration of 128μg/ml [11], indicating brevicidine is a promising antimicrobial candidate. However, before our investigations, little was known about how brevicidine exerts its potent bactericidal effect against Gram-negative pathogens. In addition, the antimicrobial activity against AMR pathogens and the therapeutic effect *in vivo* of brevicidine still needs to be investigated before it is considered for a clinical trial.

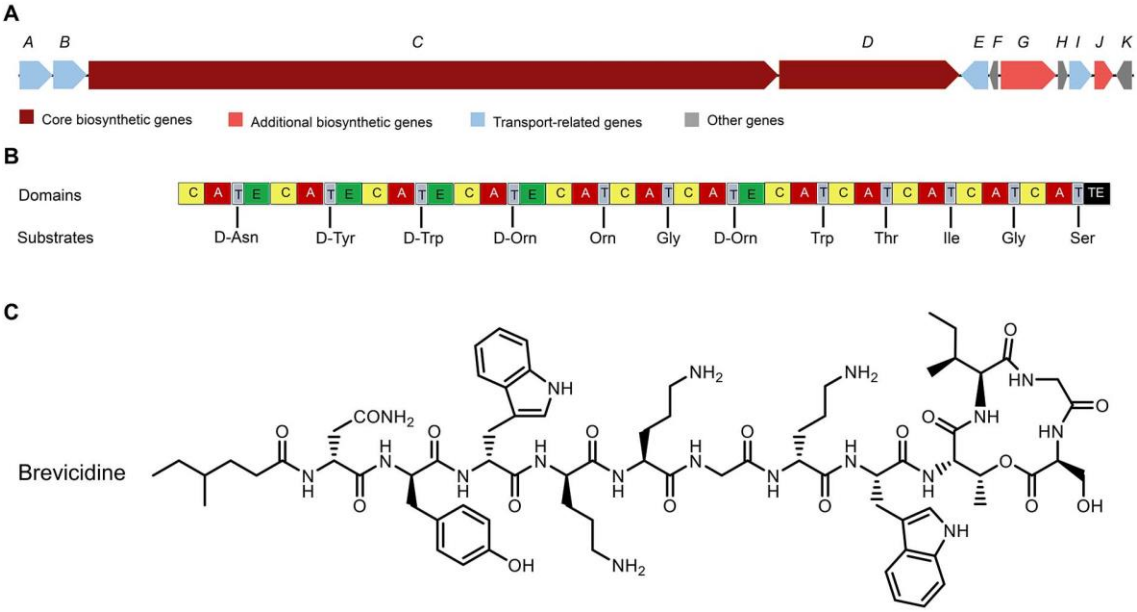

Fig 1. The structure of brevicidine and the predicted biosynthetic gene cluster. A, The non-ribosomal peptide synthetases genes harbored by the *Brevibacillus laterosporus* DSM 25 genome; **B**, the catalytic domains encoded by the gene cluster, and the substrates incorporated by the respective modules. Domains: A, adenylation; T, thiolation; C, condensation; E, epimerization; TE, thioesterase; **C**, the structure of brevicidine.

In this study, we aimed to identify the precise mechanism of action by which brevicidine kills Gram-negative pathogens. Moreover, the anti-biofilm activity against *E. coli*, the antimicrobial activity against AMR *Enterobacteriaceae*, and the *in vivo* therapeutic effect of brevicidine were also investigated. The results showed that

98 brevicidine exerts its potent bactericidal effect by interacting with lipopolysaccharide
99 (LPS) in the outer membrane, targeting phosphatidylglycerol (PG) and cardiolipin (CL)
100 in the inner membrane, and subsequently disrupting the proton motive force of
101 Gram-negative pathogens. This leads to adenosine triphosphate (ATP) synthesis
102 inhibition, nicotinamide adenine dinucleotide (NADH) and reactive oxygen species
103 (ROS) accumulation, and bacteria death. In addition, brevicidine showed potent
104 antimicrobial activity against AMR Gram-negative pathogens and good anti-biofilm
105 activity against Gram-negative pathogen. Notably, brevicidine showed a good
106 therapeutic effect in an *E. coli*-induced mouse peritonitis–sepsis model. These results
107 will pave the way for further research on the clinical applications of brevicidine.

108 Results and Discussion

109 Brevicidine shows potent antimicrobial activity against 110 antibiotic-resistant (AMR) *Enterobacteriaceae* pathogens

111 The antimicrobial activity of brevicidine against AMR *Enterobacteriaceae* pathogens
112 was measured by a MIC assay. The results show that brevicidine has potent
113 antimicrobial activity, with a MIC value of 0.5μM to 2μM (Table 1), against
114 *Enterobacteriaceae* pathogens, including the tested colistin-resistant strains and
115 multidrug-resistant strains [14]. These results indicate that brevicidine has a different
116 mechanism of action from colistin, ampiciline, ceftriaxone, cefotaxime, aztreonam,
117 gentamicin, ofloxacin, amoxicillin, streptomycin, lincomycin, doxycycline, or
118 ciprofloxacin, which makes it a more attractive antimicrobial candidate for treating
119 AMR Gram-negative pathogen infections.

120 **Table 1** MIC values of brevicidine against *Enterobacteriaceae* bacterial pathogens.

Microorganism	MIC (μM)			
	Brevicidine	**Colistin**	**Amikacin**	**Ampiciline**
Escherichia coli CVCC3749	1	2	2	> 256
Escherichia coli B2[a]	1	8	32	> 256
Escherichia coli 16QD [a]	1	8	8	> 256
Escherichia coli EPZC17-45[b]	2	2	4	> 256
Escherichia coli EPZC17-22[b]	1	1	2	> 256
Escherichia coli E21-5[b]	0.5	2	2	> 256
Escherichia coli E21-71[b]	0.5	4	4	> 256
Escherichia coli E21-75[b]	0.5	2	8	> 256
Escherichia coli E21-107[b]	0.5	1	4	> 256
Enterobacter cloacae LMG02783[c]	1	> 64	8	> 256
Klebsiella pneumoniae LMG20218	2	2	4	> 256

121 [a]*Escherichia coli* carrying mcr-1, blaNDM-5, mdfA genes, etc., which is resistant against colistin,
122 carbapenems, rifampin, etc. [b] *Escherichia coli* (clinical isolation) carrying multidrug resistance
123 genes, *Escherichia coli* EPZC17-45, resistant to ampiciline, ceftriaxone, cefotaxime, aztreonam,
124 gentamicin, doxycycline, and ciprofloxacin; *Escherichia coli* EPZC17-22, resistant to ampiciline,
125 ceftriaxone, cefotaxime, aztreonam, gentamicin, doxycycline, and ciprofloxacin; *Escherichia coli*
126 E21-5, resistant to ampiciline, amoxicillin, ceftriaxone, gentamicin, cefotaxime, streptomycin,
127 doxycycline; *Escherichia coli* E21-71, resistant to ampiciline, amoxicillin, ceftriaxone, cefotaxime,
128 doxycycline, and ciprofloxacin, and ofloxacin; *Escherichia coli* E21-75, resistant to ampiciline,
129 amoxicillin, ceftriaxone, cefotaxime, doxycycline, ofloxacin, and ciprofloxacin; *Escherichia coli*
130 E21-107, resistant to ampiciline, amoxicillin, ceftriaxone, gentamicin, cefotaxime, streptomycin,
131 doxycycline, and lincomycin. [c]*Enterobacter cloacae* carrying mcr-9 gene, which is a potent
132 colistin-resistant gene.

133 Subsequently, the safety of brevicidine was assessed by hemolytic activity (Rat and
134 mouse erythrocytes), cytotoxicity (PK-15 cell line), and toxicity (*Galleria mellonella*)
135 assays. The results showed that brevicidine, at a concentration range of 2μM to
136 128μM, neither caused cell lysis on rat erythrocytes nor on mouse erythrocytes (S1
137 Fig). Moreover, no significant cytotoxicity on PK-15 cell line was observed after
138 treatment with brevicidine at a concentration range of 0.5μM to 128μM for 48h (S2
139 Fig). Further, the *in vivo* toxicity of brevicidine was evaluated in *Galleria mellonella*.
140 The results showed that no *Galleria mellonella* died during five days post-treatment
141 with brevicidine at a concentration range of 4mg/kg to 128mg/kg. These findings

142 demonstrate that brevicidine is a promising candidate that should be further studied

143 for antimicrobial development.

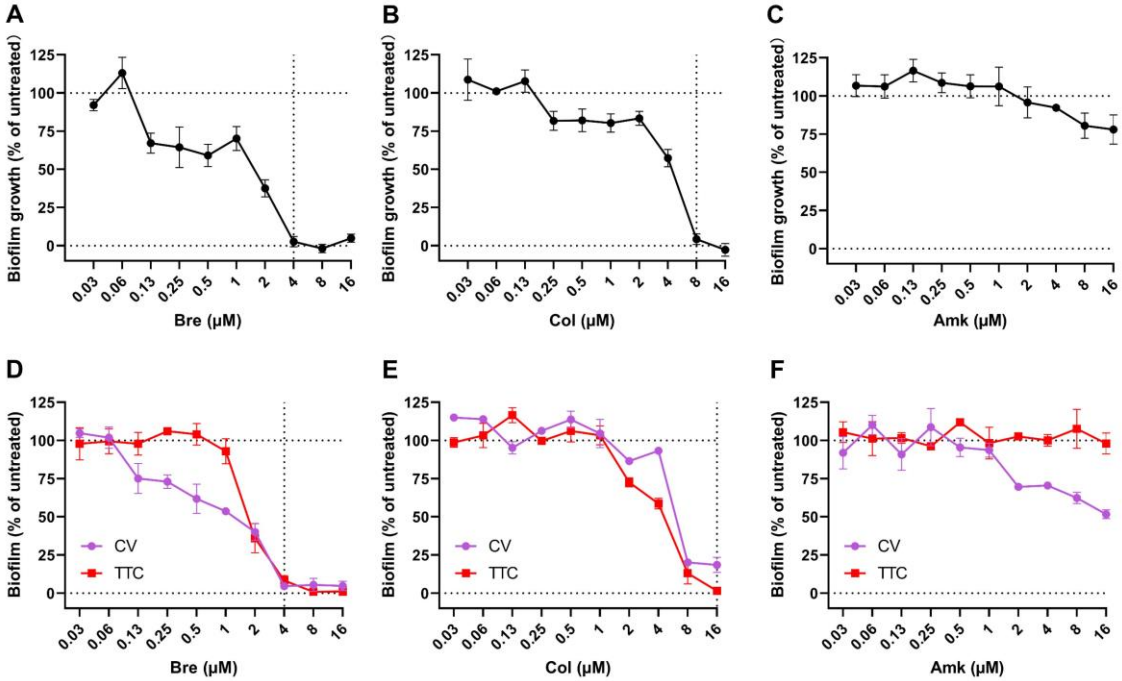

144

145 **Fig 2. Brevicidine showed potent anti-biofilm activity against *E. coli* O101. A**, Biofilm inhibition
146 of various antimicrobials (brevicidine, colistin, and amikacin) versus *E. coli* O101. Biofilm
147 inhibition was assessed by incubating the antimicrobials with bacteria in growth media for 24 h,
148 discarding the growth media and staining the adhered biomass with CV. The percentage of
149 biofilm inhibition is reported relative to untreated bacteria (defined as 100%) and sterility control
150 wells (defined as 0%). All data were presented as means ± s.d. **B**, Biofilm eradication assay results
151 for various antimicrobials (brevicidine, colistin, and amikacin) versus *E. coli* O101. Biofilm biomass,
152 quantified based on CV staining, is indicated in pink. Biofilm metabolism, quantified based on TTC
153 metabolism, is indicated in red. All data were presented as means ± s.d.

154 Brevicidine shows potent anti-biofilm activity against *E. coli*

155 Bacterial biofilm formation could increase the resistance of pathogens to
156 conventional antimicrobials, which could decrease the therapeutic effect of
157 antimicrobials [15,16]. Therefore, the anti-biofilm activity of antimicrobials plays a
158 vital role in their therapeutic effect on biofilm-formation bacterial pathogen
159 infections. In this study, the anti-biofilm activity of brevicidine against *E. coli* was
160 evaluated according to the protocol described previously [17]. Colistin (Col) was used

161 as an anti-biofilm antimicrobial control, while amikacin (Amk) was used as a control
162 antimicrobial without anti-biofilm activity. The results show that brevicidine has
163 potent anti-biofilm activity against *E. coli*, with the same 100% inhibition and
164 eradication concentration of 4μM, which is better than the anti-biofilm activity of
165 colistin against *E. coli* (Fig 2). These results demonstrate that brevicidine shows high
166 potential for the development of therapeutic antimicrobial.

167 Brevicidine dissipates the proton motive force of Gram-negative 168 bacteria

169 In a previous study, brevicidine had shown bacterial lytic activity at a concentration
170 of 10×MIC [11]. However, it did not disrupt the membrane at a concentration of 2×
171 MIC, evidenced by an atomic force microscopy assay. Therefore, the authors
172 suggested that a more in-depth mechanism study is needed to characterize the
173 targets as well as the membrane disruption effect of brevicidine [11]. In this study, to
174 investigate the killing capacity of brevicidine at concentrations of low MIC values, 4×
175 MIC, 2×MIC, and 1×MIC, a time-killing assay was performed as the previously
176 described method [18,19]. Brevicidine quickly decreased the population of *E. coli* at a
177 concentration of 4×MIC, which killed all of the tested bacteria in 1h. Interestingly,
178 the population of *E. coli* did not decrease under the treatment of brevicidine at
179 concentrations of 2×MIC and 1×MIC within 30min (Fig 3A). These results indicate
180 that brevicidine has different modes of action between high and low MIC
181 concentrations; it shows bacterial lytic activity at concentrations of 4-fold to 10-fold
182 MIC, while it does not disrupt the membrane at concentrations of 1-fold to 2-fold
183 MIC [11]. The atomic force microscopy, which was used in the previous study [11], is
184 not a common technique for investigating the membrane effect of antimicrobials

185 because of its low resolution. Therefore, in this study, we performed several
186 fluorescent probe assays, SEM assay, and TEM assay to get insight into the effect of
187 brevicidine on the Gram-negative bacterial membrane.

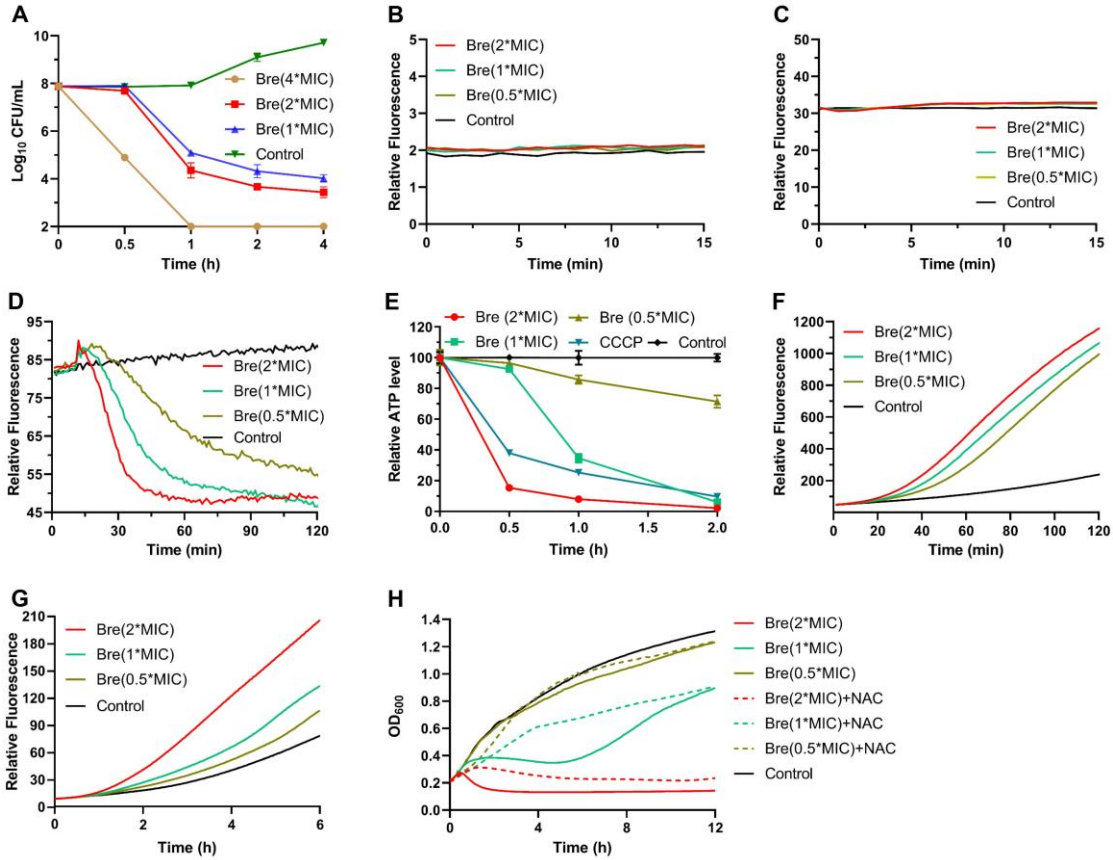

188
189 **Fig 3. Brevicidine kills Gram-negative bacteria via dissipating their proton motive force. A**,
190 time-killing curves of brevicidine at concentrations of 4×MIC, 2×MIC, and 1×MIC against *E. coli*
191 O101. **B**, *E. coli* O101 cells pretreated with propidium iodide were exposed to antimicrobial
192 peptides brevicidine at concentrations of 2×MIC, 1×MIC, and 0.5×MIC, and the extent of
193 membrane leakage was visualized as an increase in fluorescence. **C**, NPN fluorescence in *E. coli*
194 O101 cells upon exposure to brevicidine at concentrations of 2×MIC, 1×MIC, and 0.5×MIC.
195 Representative examples from three technical replicates are shown. **D**, $DiSC_3(5)$ fluorescence in *E.*
196 *coli* O101 cells upon exposure to brevicidine at concentrations of 2×MIC, 1×MIC, and 0.5×MIC.
197 Representative examples from three technical replicates are shown. **E**, ATP concentration of *E.*
198 *coli* O101 cells treated with brevicidine at concentrations of 2×MIC, 1×MIC, and 0.5×MIC. **F**,
199 Resorufin fluorescence in *E. coli* O101 cells upon exposure to brevicidine at concentrations of
200 2×MIC, 1×MIC, and 0.5×MIC. Representative examples from three technical replicates are shown.
201 **G**, Total ROS accumulation in *E. coli* O101 cells treated with brevicidine at concentrations of
202 2×MIC, 1×MIC, and 0.5×MIC. Representative examples from three technical replicates are shown.
203 **H**, Growth curves of *E. coli* O101 exposed to brevicidine at concentrations of 2×MIC, 1×MIC, and
204 0.5×MIC. Exogenous addition of NAC (6 μM) diminished the bactericidal activity of brevicidine.

205 The effect of brevicidine on the membrane integrity of Gram-negative bacteria was
206 investigated by using the fluorescent probes N-Phenyl-1-naphthylamine (NPN) and
207 propidium iodide (PI). NPN is an outer-membrane barrier permeant fluorescent
208 probe [20]. If the outer membrane is disrupted, the fluorescent probe can enter,
209 reaching the phospholipid layer and resulting in a significant increase of fluorescence.
210 The fluorescent probe PI is permeant to membrane intact bacteria, and the
211 disruption of membrane integrity can lead to a prominent increase in fluorescence
212 [18]. There was no fluorescence increase observed for both brevicidine-treated
213 NPN-containing cell suspensions and brevicidine-treated PI-containing cell
214 suspensions (Fig 3 B and C), indicating brevicidine does not disrupt the membrane
215 integrity at concentrations of 2×MIC, 1×MIC, and 0.5×MIC.
216 Although brevicidine showed no effect on the bacterial membrane integrity, it could
217 dissipate the proton motive force of bacteria as some novel antimicrobials do [21,22].
218 To test the hypothesis that brevicidine dissipated the proton motive force, a $DiSC_3(5)$
219 (3,3'-dipropylthiadicarbocyanine iodide) assay was performed. $DiSC_3(5)$ accumulates
220 in the cytoplasmic membrane of bacteria in response to the Δψ component of the
221 proton motive force [22,23]. When the transmembrane ΔpH potential of bacteria is
222 disrupted, cells compensate by increasing the Δψ, resulting in enhanced $DiSC_3(5)$
223 uptake into the cytoplasmic membrane and therefore decreased fluorescence [22,23].
224 After brevicidine treatment, the fluorescence signal of $DiSC_3(5)$ was immediately
225 reduced (Fig 3D). In addition, the descent rate of $DiSC_3(5)$ fluorescence signal was
226 displayed in a dose-dependent manner (Fig 3D). These results demonstrate that
227 brevicidine dissipats the proton motive force of bacteria.
228 The proton motive force of bacteria is essential for the generation of ATP, which is an

229 essential bioactive compound for live bacteria [24,25]. If the proton motive force of
230 bacteria is dissipated, the process of ATP biosynthesis will be inhibited or even
231 terminated. To confirm that brevicidine can dissipate the proton motive force of
232 bacteria, the ATP levels of brevicidne, at concentrations of 2×MIC, 1×MIC, and 0.5×
233 MIC, treated bacteria were measured by using the BacTiter-Glo Microbial Cell
234 Viability Assay (Promega) kit. The results showed that brevicidine decreased the ATP
235 level of bacteria as expected (Fig 3E). These results confirmed that brevicidine could
236 dissipate the proton motive force of bacteria, which is one of the mechanisms by
237 brevicidine acts as a bactericidal antimicrobial.
238 Nonfluorescent resazurin can be reduced to resorufin, a highly fluorescent compound,
239 in an NADH-dependent manner in the presence of NADH dehydrogenase [26–29].
240 Therefore, the NADH level of cells can be measured by the resazurin/NADH
241 dehydrogenase/NADH system. The dissipation of the proton motive force of bacteria
242 can result in an increase in the NADH levels of cells. To investigate the influence of
243 brevicidine on the NADH level of bacteria, a Resazurin assay was performed. The
244 results show that the NADH level of bacteria was greatly increased with the
245 treatment of brevicidine (Fig 3F). These results demonstrate that the
246 dehydrogenation of NADH can be inhibited by the addition of brevicidine, which is an
247 antimicrobial that dissipates the proton motive force of bacterial. Considering the
248 importance of the dehydrogenation of NADH to the electron transport chain of
249 bacteria, we hypothesized that brevicidine treatment could result in the
250 accumulation of ROS and thereafter kills bacteria. Therefore, the ROS levels of
251 bacteria treated with different concentrations of brevicidine were measured by using
252 a commercial kit (Beyotime, catalogue no. S0033S). The results show that brevicidine

253 increases the ROS level of bacteria (Fig 3G), which is one of the reasons that
254 brevicidine shows bactericidal activity. This was further demonstrated by growth
255 curve assay, which showed that the bactericidal activity of brevicidine was
256 attenuated by the addition of the antioxidant N-Acetyl-L-cysteine (NAC, 6 mM) (Fig
257 3H). Taking together, these results demonstrate that brevicidine exerts its bactericidal
258 activity via dissipating the proton motive force of bacteria and thereafter inhibits ATP
259 biosynthesis, inhibits the dehydrogenation of NADH, accumulates ROS in bacteria,
260 and results in bacteria death.

261 To investigate the effect of brevicidine on the cell membrane in intuitive ways, we
262 performed fluorescence microscopy, SEM, and TEM assays. The fluorescence
263 microscopy assay results are consistent with the PI and NPN assays, which
264 demonstrate that brevicidine is not an antimicrobial that kills pathogens by
265 disrupting bacteria membrane integrity (Fig 4A). Interestingly, after treatment with
266 brevicidine (1×MIC) for 15 min, the bacterial surface fold was observed (Fig 4B). In
267 addition, after treatment with brevicidine (1×MIC) for 120 min, most of the bacteria
268 were killed, evidenced by SEM and TEM images (Fig 4 B and C). These results are
269 consistent with the results of time killing assay (Fig 3A), which showed that
270 brevicidine started to kill bacteria after 30min treatments. Moreover, the
271 morphology data are also consistent that brevicidine exerts its bactericidal activity
272 via dissipating the proton motive force of bacteria because this mode of action can
273 finally cause bacteria lysis, as we observed.

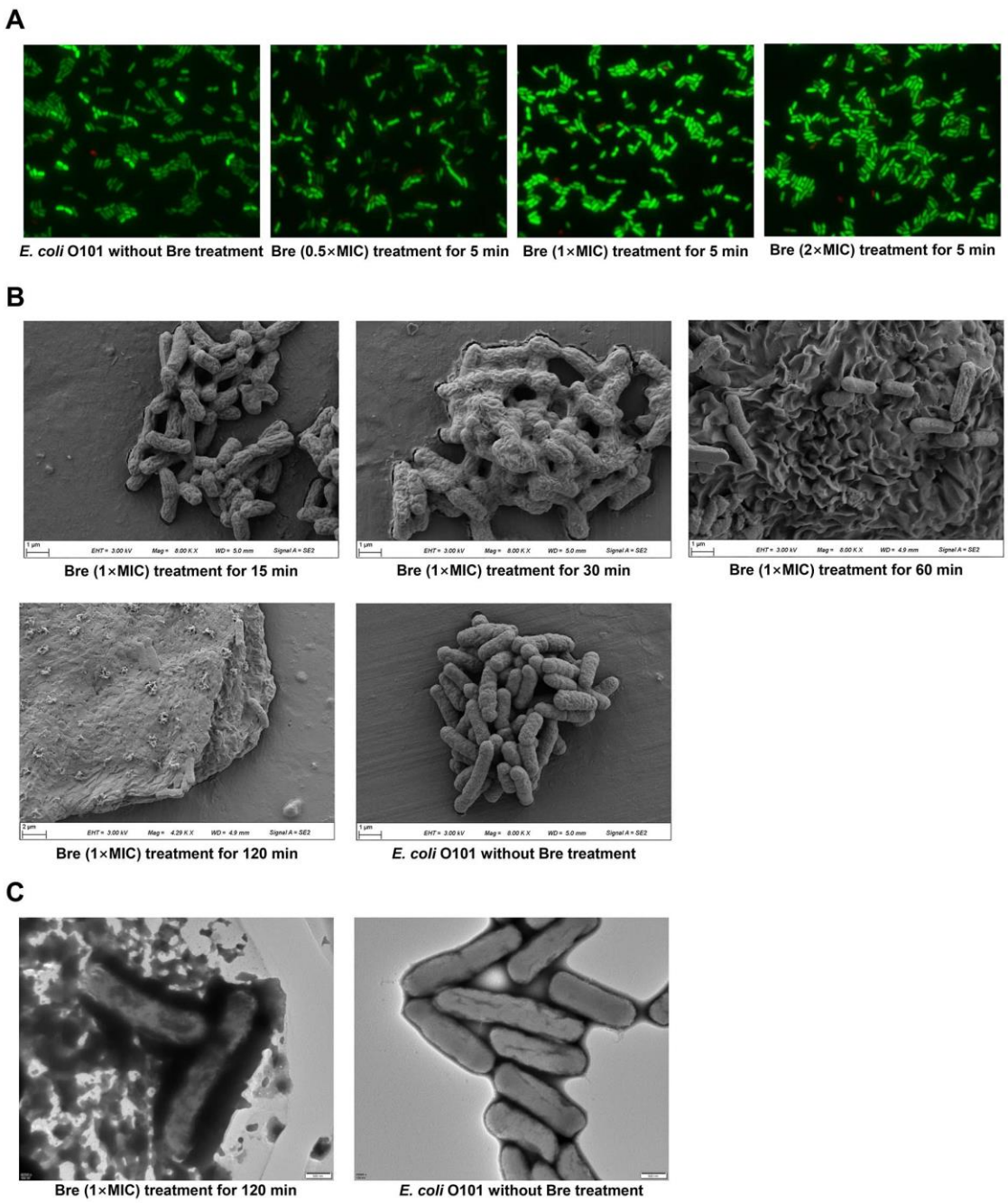

Fig 4. The morphology analysis of *E. coli* O101 under the treatment of brevicidine. A, Fluorescence microscopy images of *E. coli* O101 cells, which were challenged with brevicidine at concentrations of 2× MIC, 1× MIC, and 0.5× MIC for 5min. Green denotes a cell with an intact membrane, whereas red denotes a cell with a compromised membrane. **B**, SEM image of *E. coli* O101 cells after treatment with brevicidine at a concentration of 1× MIC for 15min, 30min, 60min, and 120min. **C**, TEM image of *E. coli* O101 cells after treatment with brevicidine at a concentration of 1× MIC for 120min.

283 **Brevicidine targets the membrane components LPS, PG, and CL**

284 As brevicidine dissipates the proton motive force of bacteria, we hypothesized that
285 brevicidine could target the component of the bacterial inner membrane. To get an
286 insight into the potential target, an agar diffusion assay was performed to investigate
287 if there is an interaction between brevicidine and LPS (outer membrane component),
288 phosphatidylethanolamine (PE, outer and inner membrane component), PG (inner
289 membrane component), or CL (inner membrane component) [30,31]. The main
290 component of mammalian cellular membrane phosphatidylcholine (PC) was used as
291 a control. The results show that the addition of PC or PE did not attenuate the
292 antimicrobial activity of brevicidine (Fig 5A). In contrast, the antimicrobial activity
293 was completely abolished by the addition of LPS, PG, or CL (Fig 5A). Subsequently, to
294 investigate the dose-dependent effect of LPS, PG, or CL on the antimicrobial activity
295 of brevicidine, a MIC assay was performed with different concentrations of LPS, PG,
296 CL, PC, or PE. The MIC value of brevicidine had no changes with the addition of PC
297 and PE, suggesting there is no interaction between brevicidine and PE (or PC) (Fig 5B).
298 This could explain why brevicidine targets the Gram-negative bacteria but has low
299 cytotoxicity to mammalian cells (S2 Fig) [11]. LPS, PG, and CL decreased the
300 antimicrobial activity of brevicidine in a dose-dependent manner, and the MIC value
301 of brevicidine increased 8-fold, 16-fold, and 64-fold by the addition of 128μg/ml of
302 LPS, PG, and CL, respectively (Fig 5B). These results indicate that brevicidine could
303 bind to the cell membrane components LPS, PG, and CL.

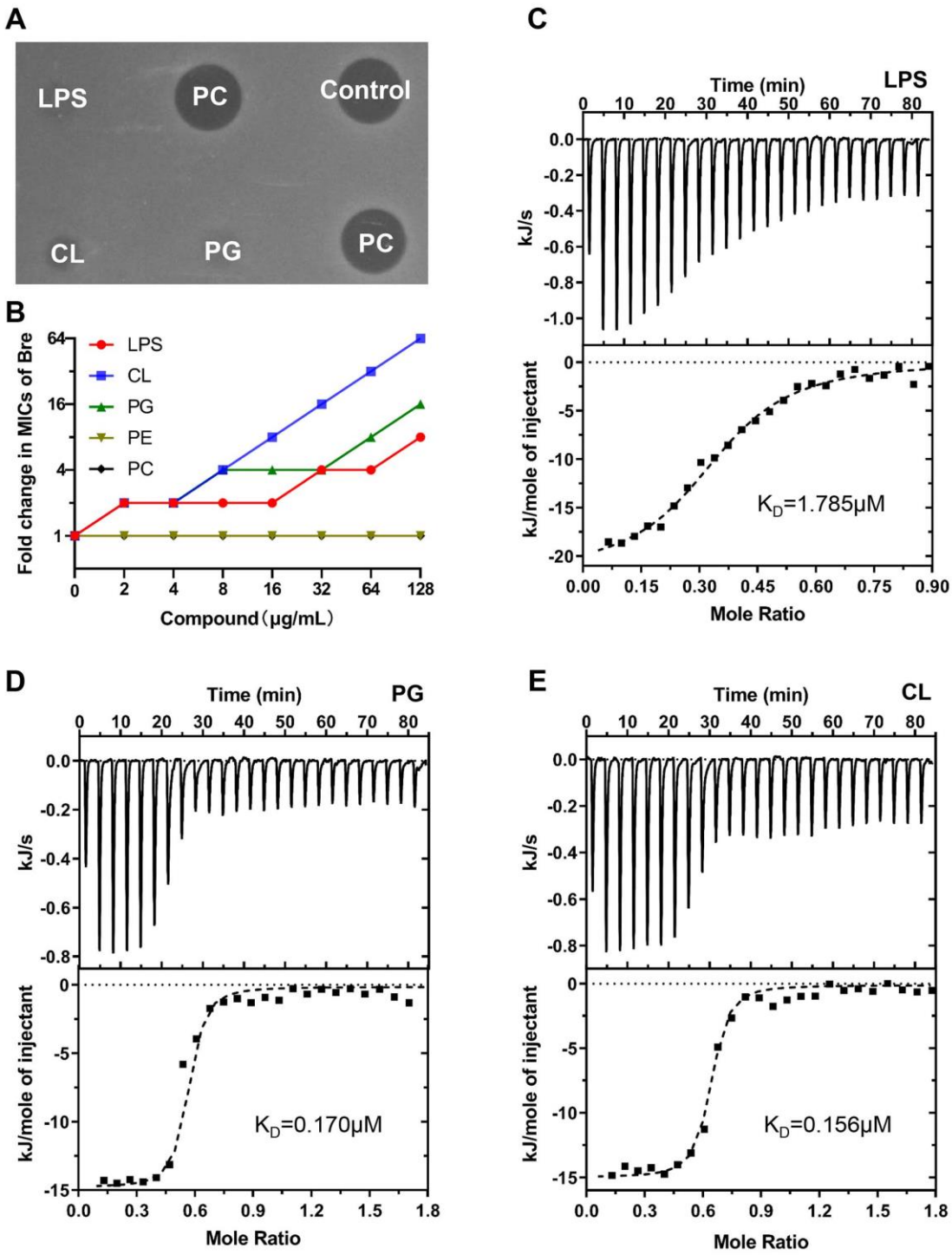

Fig 5. Brevicidine targets the membrane components LPS, PG, and CL. A, Exogenous addition of LPS, PG, or CL abolishes the antibacterial activity of brevicidine against *E. coli* O101. Inhibition zones of the mixtures of 1 nmol of brevicidine and 4 mmol of PC, LPS, PE, PG and CL, against *E. coli* O101 for overnight incubation at 37 °C. **B**, Increased MICs of brevicidine against *E. coli* O101 in the presence of LPS, PG and CL, ranging from 0 μg/ml to 128 μg/ml, based on MIC assays. **C**, ITC analysis of the interaction between brevicidine and LPS. **D**, ITC analysis of the interaction between brevicidine and PG. **E**, ITC analysis of the interaction between brevicidine and CL. The K_D values of brevicidine to LPS, PG and CL were calculated using the Nano Analyze Software (Waters LLC).

314 To gain an insight into the interaction between brevicidine and LPS, PG, or CL, an ITC
315 measurement was performed. The results show that CL and PG showed comparable
316 binding affinity to brevicidine, with K_D values of 0.156 μM and 0.170 Mm (Fig 5 C and
317 D), respectively. Notably, CL and PG have much stronger (approximately 10-fold
318 stronger) binding affinity to brevicidine than LPS, which has a K_D value of 1.785 μM
319 (Fig 5E). These results demonstrate that brevicidine has multiple targets on the
320 bacteria, which is good for inhibiting the development of bacterial antibiotic
321 resistance. Together, the observed results demonstrate that brevicidine exerts its
322 bactericidal activity via interacting with LPS in the outer membrane and targeting CL
323 and PG in the inner membrane, and thereafter dissipating the proton motive force of
324 bacteria.

325 **Brevicidine inhibits the oxidative phosphorylation and protein**
326 **synthesis processes of *E. coli***

327 To gain an insight into the antimicrobial mechanism of brevicidine, transcriptome
328 analysis was performed on *E. coli* treated with or without brevicidine at a
329 concentration of 0.5μM. The whole distribution of differentially expressed genes
330 (DEGs) is shown in Fig 6A. When padj value<0.05 and log2(FoldChange)>0, among
331 4622 genes, 587 were upregulated and 622 were downregulated, and 3413 genes
332 were not significantly changed (Fig 6A). Subsequently, Kyoto Encyclopedia of Genes
333 and Genomes (KEGG) enrichment analysis was performed on the genes that had
334 significantly expression changes. The results showed that ribosome, oxidative
335 phosphorylation, and aminoacyl-tRNA biosynthesis pathways were significantly (padj

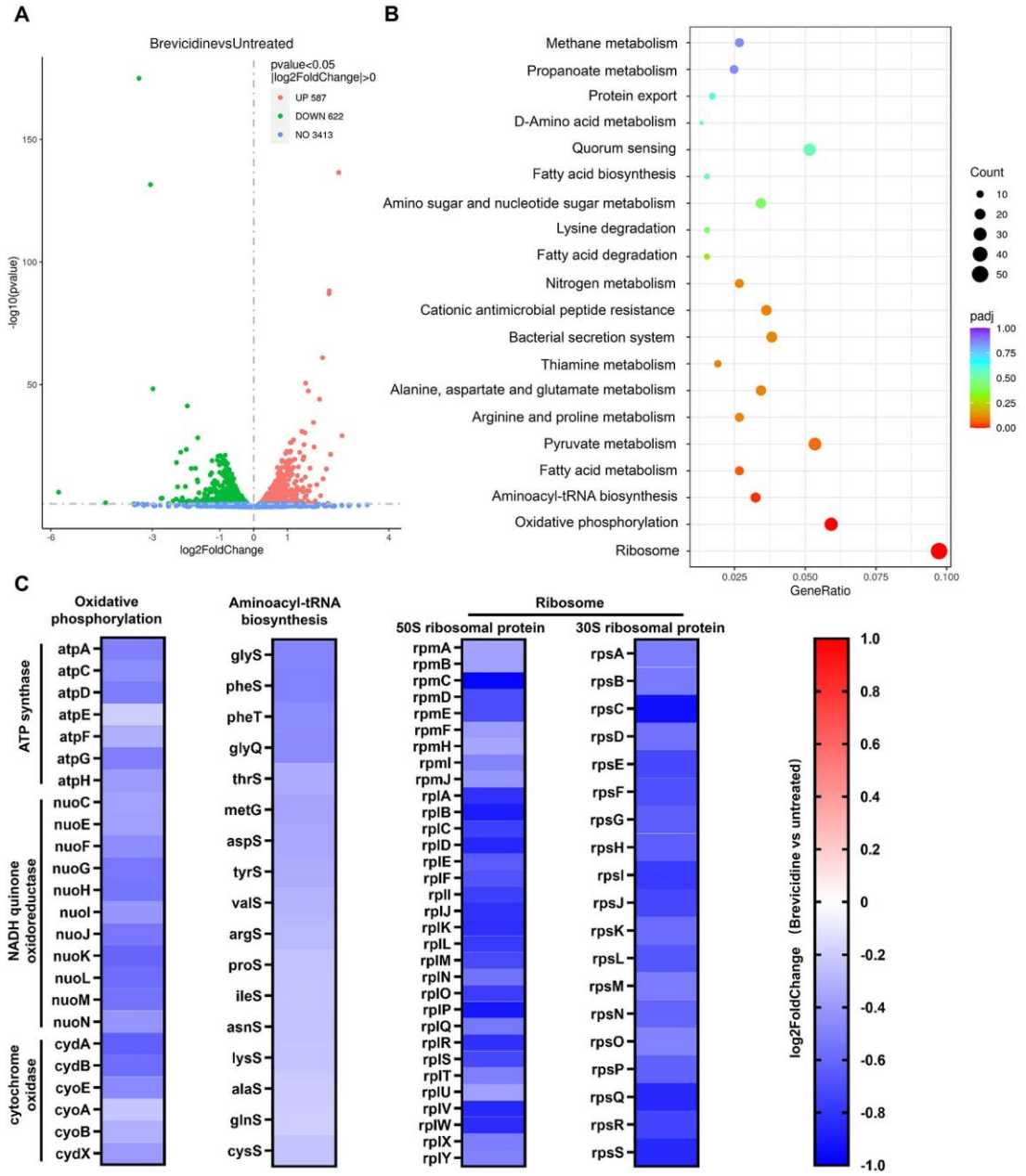

Fig 6. Transcriptome analysis of *E. coli* O101 under the treatment of brevicidine (0.5 μM) for 1 h. **A**, The volcano map of DEGs. The abscissa represents the multiple changes of gene expression between brevicidine treated and untreated *E. coli* O101; the ordinate represents the statistical significance of the change of gene expression (pvalue<0.05 |log2FoldChange|>0). **B**, Scatter plot of KEGG pathway enrichment analysis of DEGs (Brevicidine vs untreated). The vertical axis represents the KEGG enrichment analysis pathway name, and the horizontal axis represents the gene ratio of the genes in the pathway. The size of the dots indicates the number of DEGs in the pathway, and the color of the dots corresponds to different padj value ranges. **C**, Genes involved in oxidative phosphorylation, ribosome, and aminoacyl-tRNA biosynthesis were identified as significantly different between the treatment of brevicidine and untreated, with pvalue values <0.05 and log2FoldChange <0 in expression level. All genes that had significantly changes were down-regulated in oxidative phosphorylation, ribosome, and aminoacyl-tRNA biosynthesis pathways. All data are presented as means (n= 3 biological replicates).

value<0.05) affected by brevicidine treatment (Fig 6B). After *E. coli* exposure to brevicidine for 1h oxidative phosphorylation related genes including ATP synthase, NADH-quinone oxidoreductase, and cytochrome oxidase were significantly downregulated (Fig 6C). This change would contribute to the lower level of ATP, higher level of NADH and ROS of the brevicidine treated cells. The downregulated tRNA ligase and ribosome synthesis metabolism indicate that the protein synthesis process was inhibited by brevicidine treatment.

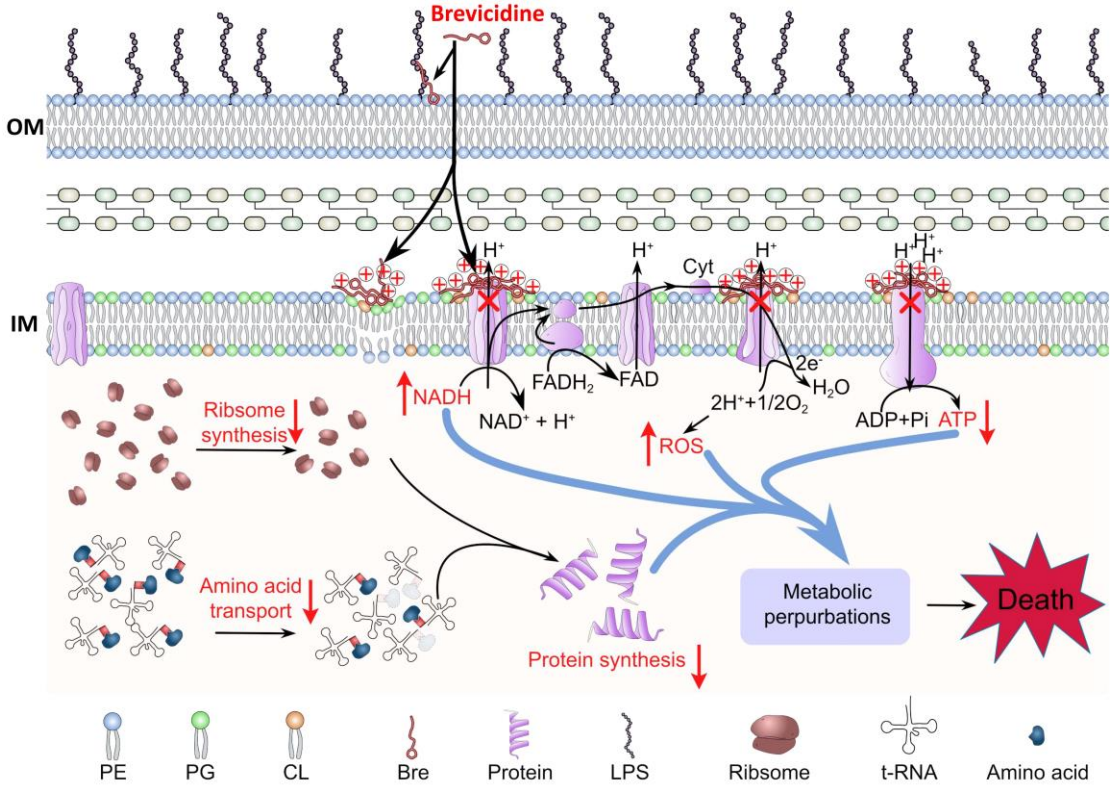

Fig 7. Scheme of the mechanism of action brevicidine against *E. coli*. Brevicidine exerts its bactericidal activity via interacting with LPS in the outer membrane (OM) and targeting CL and PG in the inner membrane (IM), and thereafter dissipating the proton motive force of the bacteria. This results in metabolic perturbation, including decreases in the intracellular ATP level, inhibits the dehydrogenation of NADH and accumulates ROS in bacteria. In addition, transcriptome analysis results showed that brevicidine inhibits the synthesis of t-RNA ligase (essential for amino acid transport) and ribosome protein synthesis, which can result in protein synthesis inhibition. All these actions together lead to the death of Gram-negative pathogens.

368 Collectively, our findings demonstrate that brevicidine exerts its bactericidal activity
369 via interacting with LPS in the outer membrane and targeting CL and PG in the inner
370 membrane, and thereafter dissipation of the proton motive force of bacteria. This
371 can result in metabolic perturbation, including inhibits ATP biosynthesis, inhibits the
372 dehydrogenation of NADH, accumulates ROS in bacteria, and inhibits protein
373 synthesis (Fig 7).

374 Brevicidine showed a good therapeutic effect in a mouse 375 peritonitis–sepsis model

376 Given the attractive mode of action and potent antimicrobial and anti-biofilm activity
377 of brevicidine, we investigated its potential as a therapeutic in a mouse
378 peritonitis–sepsis model (Fig 8A). Mice were infected intraperitoneally with *E. coli* at
379 a dose that leads to 80% of death. At 1h post-infection, brevicidine was introduced
380 intraperitoneally at single doses ranging from 10mg/kg to 40mg/kg. All
381 brevicidine-treated mice were survived (Fig 8B). Consistently, the bacterial load in
382 different organs of mice significantly reduced under brevicidine treatment in a
383 dose-dependent manner at either 1 or 7 days post-infection (Fig 8 C-G, and S3 Fig).
384 These results are consistent with the previous study, which showed that brevicidine
385 had good antimicrobial activity in a mouse thigh model [11]. Together, these findings
386 demonstrate the potential of brevicidine as a novel therapeutic antimicrobial in AMR
387 Gram-negative pathogen infections, in particular, AMR *Enterobacteriaceae* pathogen
388 infections.
389

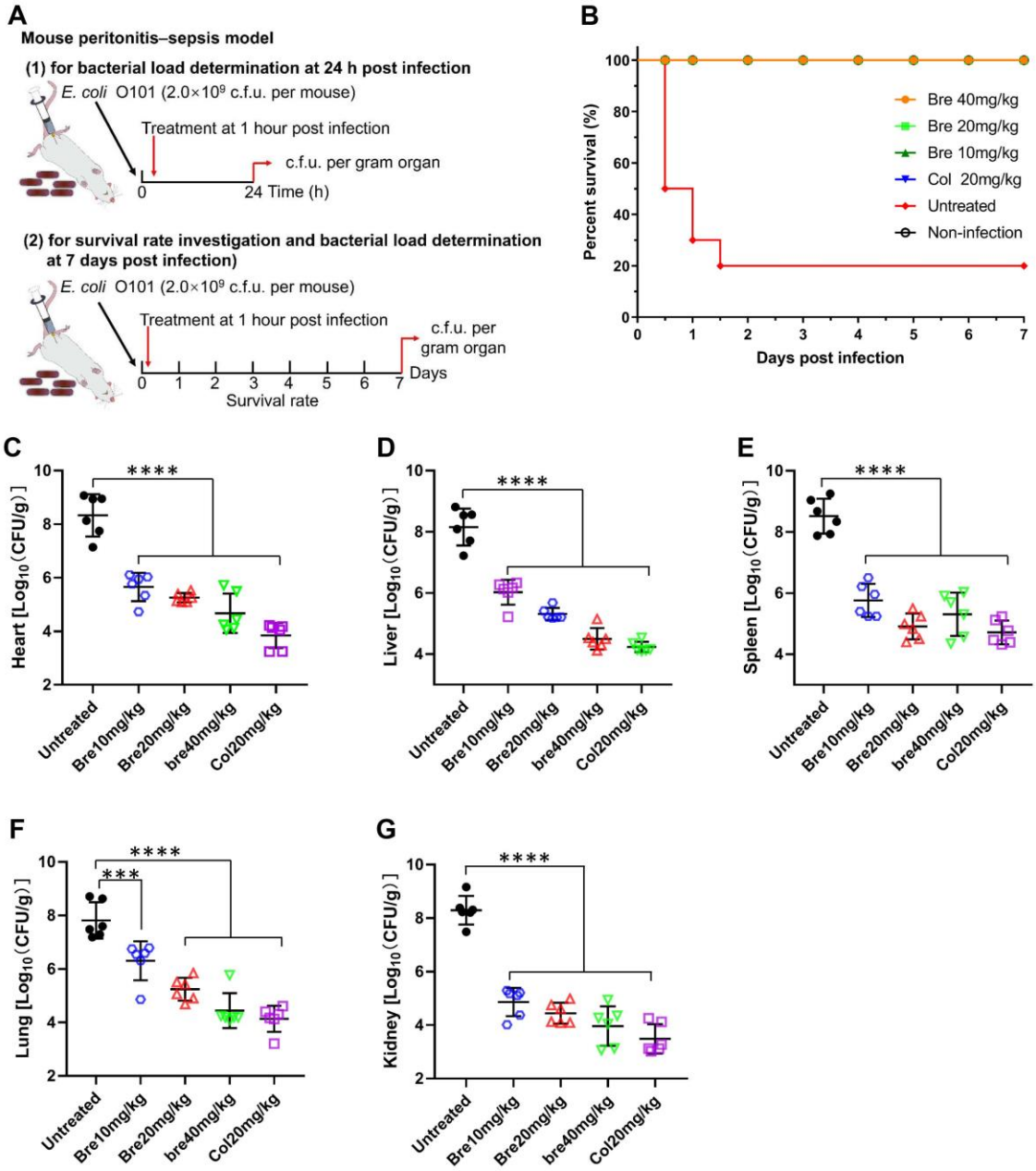

Fig 8. Brevicidine showed a good therapeutic effect in a mouse peritonitis–sepsis model. A, Scheme of the experimental protocol for the mouse peritonitis–sepsis model. **B**, Survival rates of mice in the mouse peritonitis–sepsis model (n= 10). Increased survival rates of mice over 7 d by a dose that leads to 80% of death of *E. coli* O101 (2.0×10^9 c.f.u.), treated with brevicidine (10 mg per kg, 20 mg per kg, or 40 mg per kg) or with colistin (20 mg per kg). **C to G**, Brevicidine significantly reduced the bacterial load of organs of the peritonitis-sepsis mouse. At 24h post-infection, the survived mice (n = 6) were euthanized by cervical dislocation. Bacterial loads (Log10 CFU per gram of *E. coli* O101) of the heart (**C**), liver (**D**), spleen (**E**), lung (**F**) and kidney (**G**) were counted. All data were presented as means ± SD (n = 6). Correlation analyses were evaluated by Pearson r2, ns: ***$p < 0.01$ and ****$p < 0.001$ vs. untreated group.

403 ## Conclusions

404 AMR poses a major threat to human health around the world; many bacterial
405 infections have become increasingly difficult, or even impossible, to treat with
406 conventional antimicrobials. Therefore, new first-in-class antibiotics, operating via
407 novel modes of action, are desperately-needed. Here, we show that brevicidine has
408 potent antimicrobial activity against AMR *Enterobacteriaceae* pathogens, with a MIC
409 value range of 0.5μM to 2μM. In addition, brevicidine showed potent anti-biofilm
410 activity against the *Enterobacteriaceae* pathogens, with the same 100% inhibition
411 and eradication concentration of 4μM. Mechanistic studies showed that brevicidine
412 exerts its potent bactericidal activity via interacting with LPS in the outer membrane,
413 targeting PG and CL in the inner membrane, and dissipating the proton motive force
414 of bacteria. This results in metabolic perturbation, including inhibition of ATP
415 biosynthesis, inhibition of the dehydrogenation of NADH, accumulation of ROS in
416 bacteria, and inhibition of protein synthesis (Fig 7). Lastly, brevicidine showed a good
417 therapeutic effect in a mouse peritonitis–sepsis model. Our findings pave the way for
418 further research on clinical applications of brevicidine, to combat the prevalent
419 infections caused by AMR Gram-negative pathogens worldwide.

420 ## Materials and Methods

421 ### Ethical approval

422 The animal experiment protocol was approved by the Animal Ethical and welfare
423 Committee of Sichuan Agricultural University [permission number 20220087].

424

425 **Bacterial strains used and growth conditions**

426 Bacterial strains used in this study are listed in S1 Table. All bacterial strains were
427 inoculated in LB and incubated at 37°C with aeration at 220 rpm for preparing the
428 overnight cultures.

429 **Purification of brevicidine**

430 Methods for the purification of brevicidine have been described in detail previously
431 [12]. The matrix-assisted laser desorption ionization-time-of-flight mass spectrometry
432 data is shown in S4 Fig, which is showing the correct molecular weight of the purified
433 brevicidine.

434 **Minimum inhibitory concentration (MIC) assay**

435 MIC values of antimicrobials against the tested bacterial pathogens were determined
436 according to the standard guidelines [32]. Briefly, cell concentration was adjusted to
437 approximately 5×10^5 cells per ml in cation-adjusted Mueller-Hinton broth (MHB).
438 Subsequently, antimicrobials were added to the above bacterial cultures at different
439 concentrations. After 24h of incubation at 37°C, the MIC value was defined as the
440 lowest concentration of antimicrobial with no visible growth.

441 For measuring the MIC values of antimicrobials against indicator strains in the
442 presence of cell membrane components, MHB was replaced with MHB containing
443 different concentrations of cell membrane components, and the effect of these two
444 conditions was compared.

445 **Hemolytic activity assay**

446 Hemolytic activity assay was performed as the method described in previous studies

447 [11,19]. Briefly, fresh rat or mouse blood was washed with 0.1 M PBS three times,
448 and the erythrocytes were collected. Subsequently, brevicidine was added at final
449 concentrations of 128, 64, 32, 16, 8, 4, 2 and 0 μM in PBS containing 2% (v/v)
450 erythrocytes. The cells were incubated at 37 °C for 1 h and centrifuged for 5 min at
451 5000 g. The supernatants were transferred to a 96-well plate, and the absorbance
452 was measured at a wavelength of 570 nm with a Thermo Scientific Varioskan™ LUX
453 multimode microplate reader. The absorbance relative to the positive control, which
454 was treated with 10% Triton X-100, was defined as the percentage of hemolysis.
455 Representative examples from three technical replicates are shown.

456 **Mammalian cytotoxicity**

457 The cytotoxicity of brevicidine was evaluated on a porcine kidney cell line (PK-15) by
458 using the cell counting kit-8 (CCK-8; Dojindo Molecular Technologies, Kumamoto,
459 Japan) [33]. PK-15 cells (in Dulbecco's Modified Eagle's medium supplemented with
460 10% Fetal Bovine Serum) were seeded into 96-well plates and incubated at 37 °C with
461 5% CO_2. After 24 h, the medium was replaced with a fresh medium (DMEM with 2%
462 FBS, 100 μL per well) containing different concentrations of brevicidine [33]. After
463 48 h incubation, the CCK-8 reagent was added to the cultures according to the
464 manufacturer's instructions, and the plates were incubated at 37 °C for 2 h with 5%
465 CO_2. Subsequently, the absorbance values were measured by using a Varioskan™ LUX
466 multimode microplate reader (Thermo Fisher Scientific) at 450 nm.

467 ***In vivo* toxicity in the *Galleria mellonella***

468 A toxicity analysis was performed on *G. mellonella* according to previously described
469 protocols [34,35]. The worms, 300 to 350 mg per worm, were stored in the dark at

470 4 °C with wood shavings before use. For each treatment, 10 healthy worms were
471 placed in Petri dishes with filter paper on the bottom, and 10 µl of the compound
472 was injected into the worm through the last left proleg. The final dosages injected
473 into the worms were 4, 8, 16, 32, 64, and 128 mg/kg. NaCl 0.9% was used as a
474 negative control. The inoculated worms were incubated at 37 °C for 5 d, and record
475 the mortality daily.

476 **Biofilm inhibition assay**

477 Biofilm inhibition assay was performed according to a previously described protocol
478 [17]. Briefly, an overnight culture of *E. coli* O101 was diluted 100-fold in tryptone soy
479 broth (TSB) and incubated at 37 °C with aeration at 220 r.p.m. Bacteria were grown to
480 an OD_{600} of 0.8, and then the concentration of cells was adjusted to an OD_{600} of 0.04
481 in TSB. The cell suspension was added to a 96-well plate, and antimicrobials were
482 added at different final concentrations. After incubation at 37 °C for 24 h, the wells
483 were washed with MiliQ water three times, and the adhered biomasses were stained
484 with 105 µl of a 0.1% crystal violet (CV) (wt/vol) solution. The plate was placed on a
485 low-speed orbital shaker and allowed to stain at room temperature for 30 min.
486 Subsequently, the plate was washed with MiliQ water three times, and then 70%
487 (vol/vol) ethanol was added to the wells (110 µl per well) and incubated for 30 min at
488 room temperature with gentle shaking. The absorbance was measured by using a
489 Thermo Scientific Varioskan™ LUX multimode microplate reader with a wavelength of
490 595 nm. The inhibition rates were calculated by the raw CV absorbance values from
491 each growth condition vs the raw CV absorbance value of normally grown biofilm.
492 Representative examples from three technical replicates are shown.

493 **Biofilm eradication assay**

494 Biofilm eradication assay was performed according to a previously described protocol
495 [17]. Briefly, an overnight culture of *E. coli* O101 was diluted 100-fold in tryptone soy
496 broth (TSB) and incubated at 37 °C with aeration at 220 r.p.m. Bacteria were grown to
497 an OD_{600} of 0.8, and then the concentration of cells was adjusted to an OD_{600} of 0.04
498 in TSB. The cell suspension was added to 96-well plates and incubated at 37 °C for 24
499 h. After washing the wells with TSB three times, antimicrobials were added to the
500 wells at different concentrations, and the plates (one for CV staining, the other one
501 for TTC staining) were incubated at 37 °C for 24 h. For measuring the metabolic
502 activity of biofilm, a final concentration of 0.05% TTC was added to wells with
503 antimicrobials. Subsequently, the adhered biomasses were measured as the method
504 described in the biofilm inhibition assay. After washing all the wells of the TTC plate
505 three times with distilled water, dimethyl sulfoxide (DMSO) was added to the wells at
506 205 μl per well. After that, the plate was placed on an orbital shaker rotating at low
507 speed and mixed at room temperature for 30 min. The absorbance of the TTC plate
508 was measured by using a Thermo Scientific Varioskan™ LUX multimode microplate
509 reader with a wavelength of 500 nm. The biofilm eradication (Biomass and
510 metabolism) rate was calculated by the method described in the previous study [17].
511 Representative examples from three technical replicates are shown.

512 **Time-dependent killing assay**

513 The time-dependent killing assay was performed according to the procedure
514 described previously [18,19]. An overnight culture of *E. coli* O101 was diluted
515 100-fold in MHB and incubated at 37 °C with aeration at 220 r.p.m. Bacteria were

516 grown to an OD of 0.6, and then the concentration of cells was adjusted to 7.6×10^7
517 cells per mL. Bacteria were then challenged with antimicrobials at concentrations of
518 1×MIC, 2×MIC, or 4×MIC in glass culture tubes at 37 °C with aeration at 220 r.p.m.
519 Bacteria not treated with antimicrobials were used as normal growth control. At
520 desired time points, two hundred µl aliquots were taken, centrifuged at 5,000 g for 5
521 min, and resuspended in 200 µl of MHB. Ten-fold serially diluted samples were plated
522 on MHA plates. After incubation at 37 °C for 24 h, colonies were counted, and the
523 colony forming units (c.f.u.) per ml were calculated. Each experiment was performed
524 in triplicate.

525 **Membrane integrity assay**

526 A fresh culture of *E. coli* O101 was pelleted at 5,000 g for 5 min and washed three
527 times with MHB. The cell density was normalized to an OD_{600} of 0.2, loaded with
528 propidium iodide (final concentration 2.5 µg per ml), and incubated for 5 min in the
529 dark for probe fluorescence to stabilize. After the cell suspension was added to a
530 96-well microplate, brevicidine was added to final concentrations of 2×MIC, 1×MIC,
531 or 0.5×MIC, with the antimicrobials added after ~30 s, and fluorescence was
532 monitored for 15 min. The excitation and emission wavelengths on the fluorescence
533 spectrometer were adjusted to 533 nm and 617 nm, respectively. Representative
534 examples from three technical replicates are shown.

535 **Outer membrane permeability assay**

536 The integrity of the outer membrane was investigated with the fluorescent probe
537 N-Phenyl-1-naphthylamine (NPN, Aladdin). A fresh culture of *E. coli* O101 was
538 pelleted at 5,000 g for 5 min and washed three times with 10 mM HEPES containing

539 10 mM glucose (GHEPES, pH 7.2). The cell density was normalized to an OD_{600} of 0.2
540 in GHEPES, loaded with NPN (final concentration 30 μM), and incubated for 30 min in
541 the dark for probe fluorescence to stabilize. After the cell suspension (190 μL) was
542 added to a 96-well microplate, brevicidine (10 μL) was added to final concentrations
543 of 2×MIC, 1×MIC, or 0.5×MIC, with the antimicrobials added after ~30 s, and
544 fluorescence was monitored for 15 min. The excitation and emission wavelengths on
545 the fluorescence spectrometer were adjusted to 350 nm and 420 nm, respectively.
546 Representative examples from three technical replicates are shown.

547 **Fluorescence microscopy assay**

548 This assay was performed according to the procedure described previously [29,36]. *E.*
549 *coli* O101 was grown to an OD_{600} of 0.6 in MHB. The culture was pelleted at 5,000 g
550 for 5 min and washed with MHB three times. After normalization of the cell density
551 to an OD_{600} of 0.2 in MHB, brevicidine was added to a final concentration of 2×MIC,
552 1×MIC or 0.5×MIC. After incubation at 37 °C for 5min, cells were collected by
553 centrifugation. Subsequently, SYTO® 9 and propidium iodide (LIVE/DEAD Baclight
554 Bacterial Viability Kit, Invitrogen) were added to the above cells. After incubation at
555 room temperature for 15 min, cells were washed three times with MHB. Then the
556 cell suspensions were loaded on 1.5 % agarose pads and analyzed by Nikon 80i
557 (Japan) microscope.

558 **$DiSC_3(5)$ assay**

559 DiSC3(5) assay was adapted from previously described procedures [22,29]. Briefly, a
560 fresh *E. coli* O101 culture was pelleted at 5,000 g for 5 min and washed three times
561 with MHB. The cell density was normalized to an OD_{600} of 0.2, loaded with 6 μM

562 $DiSC_3(5)$ dye (3,3'-dipropylthiadicarbocyanine iodide), and incubated for 30 min in
563 the dark for probe fluorescence to stabilize. Subsequently, the cell suspension was
564 added to a 96-well microplate and incubated for 30 min. After antimicrobials were
565 added at final concentrations of 2×MIC, 1×MIC, or 0.5×MIC, with the antimicrobials
566 added after ~30 s, fluorescence was monitored for 100 min. The excitation and
567 emission wavelengths on the fluorescence spectrometer were adjusted to 622 nm
568 and 670 nm, respectively. Representative examples from three technical replicates
569 are shown.

570 **Resazurin assay**

571 Nonfluorescent resazurin can be reduced to resorufin, a highly fluorescent compound,
572 in an NADH-dependent manner in the presence of NADH dehydrogenase [26–29].
573 Therefore, the resazurin/NADH dehydrogenase/NADH system can be used to detect
574 the NADH level of cells. *E. coli* O101 cells were grown in MHB until the OD_{600} reached
575 0.2. Resazurin was added to the cell culture at a final concentration of 100 µg per ml.
576 Brevicidine was added to final concentrations of 2×MIC, 1×MIC, or 0.5×MIC. Milli Q
577 water was used as an untreated control. Fluorescence was recorded by using a
578 Thermo Scientific Varioskan™ LUX multimode microplate reader with an emission
579 wavelength of 560 nm. Representative examples from three technical replicates are
580 shown.

581 **ATP determination**

582 The ATP levels were determined using a BacTiter-Glo Microbial Cell Viability Assay kit
583 (Promega). A fresh culture of *E. coli* O101 was pelleted at 5,000 g for 5 min and
584 washed three times with MHB. The cell density was normalized to an OD_{600} of 0.2,

585 loaded with brevicidine at final concentrations of 2×MIC, 1×MIC, or 0.5×MIC. At
586 desired time points, 100 μl of cell culture were taken out, mixed with 100 μl
587 BacTiter-Glo reagent, and incubated for 5 minutes at room temperature.
588 Luminescence was measured with an Infinite M2000pro Microplate reader (Tecan).
589 CCCP (40 μg/mL) was used as a positive control. The relative ATP levels were
590 calculated using the measured Luminescence values vs the Luminescence value of
591 untreated cells at relative time points.

592 **Reactive oxygen species (ROS) measurement**

593 The levels of ROS in *E. coli* O101 treated with different concentrations of brevicidine
594 were measured by 10 μM of 2′,7′-dichlorofluorescein diacetate (DCFH-DA), following
595 the manufacturer's instruction (Beyotime, catalogue no. S0033S). Briefly, a fresh
596 culture of *E. coli* O101 was pelleted at 5,000 g for 5 min and washed three times with
597 MHB. The cell density was normalized to an OD_{600} of 1.0, loaded with DCFH-DA at a
598 final concentration of 10 μM, and the mixture incubated at 37 °C for 30 min. After
599 washing with MHB three times, 190 μl of probe-labeled bacterial cells were added to
600 a 96-well plate, and then 10 μl of brevicidine. Fluorescence was recorded by using a
601 Thermo Scientific Varioskan™ LUX multimode microplate reader with the excitation
602 wavelength at 488 nm and the emission wavelength at 525 nm. The antioxidant
603 N-Acetyl-L-cysteine (NAC, 6 mM) was used as a control to neutralize the production
604 of ROS.

605

606

607 **Scanning electron microscopy (SEM) and transmission electron**

608 **microscopy (TEM) assays**

609 The morphology of 1μM brevicidne treated *E. coli* O101 was recorded in vacuum on a
610 ZEISS Gemini SEM300 with an acceleration voltage of 3kV. For TEM measurements,
611 samples were prepared by delivering 2μl of 1μM brevicidine treated *E. coli* O101
612 suspension to carbon-coated copper grids and dried in a vacuum system. The
613 morphology was obtained under a JEM-2100Plus Electron Microscope using an
614 acceleration voltage of 120kV.

615 **Spot-on-lawn assay**

616 An overnight cultured *E. coli* O101 was added to 0.7% MHA (w/v, temperature 42 °C)
617 at a final concentration of 0.25% (v/v), and then the mixture was poured onto the
618 plates, with 20 mL for each 15 cm diameter circular plate. Subsequently, a
619 spot-on-lawn assay was used to analyze the antimicrobial activity of brevicidine in
620 the presence of cell membrane components [18]. In short, 20 μL brevicidine (50 μM)
621 containing 200 μM lipopolysaccharides (LPS, Solarbio, catalogue no. L8880, ≥98%),
622 L-α-phosphatidylcholine, (PC, Aladdin, catalogue no. L130331, ≥99%),
623 L-α-phosphatidylglycerol (PG, Aladdin, catalogue no. L130372; ≥99%),
624 L-α-phosphatidylethanolamine (PE, Aladdin, catalogue no. L130310; ≥99%) or
625 Cardiolipin (CL, Aladdin, catalogue no. B130227;≥99%) was loaded to the agar plate
626 that contains indicator strain. After the brevicidiene/cell membrane component
627 mixture solution drops had dried, the plates were transferred to a 37 °C incubator for
628 overnight incubation.

629 **Isothermal Titration Calorimetry (ITC) assay**

630 ITC was performed with the Low Volume NanoITC (TA Instruments) at 25°C to

631 determine the interaction between brevicidine and LPS, PG, or CL. Brevicidine was
632 diluted in a buffer (20 mM HEPES, pH7.0) to a final concentration of 50 μM. Samples
633 were degassed before use. The chamber was filled with 300 μL of the brevicidine
634 solution, and LPS (250μM), PG (500μM), or CL (500μM) was titrated into the
635 chamber at a rate of 1.96 μL/200 s with a stirring rate of 300 rpm. The control
636 experiment was performed with 20 mM HEPES titration to 50 μM brevicidine. The K_D
637 values of brevicidine to LPS, PG, or CL were calculated using the Nano Analyse
638 Software (Waters LLC).

639 **Transcriptome analysis of E. coli O101 treated with brevicidine**

640 Three replicates of overnight bacteria cultures were diluted at 1:100 in MHB and
641 grown at 37˚C with aeration at 220rpm. Bacteria were grown to an OD_{600} of 0.4, and
642 then the concentration of cells was adjusted to an OD_{600} of 0.2 in MHB. Subsequently,
643 the bacteria were treated with brevicidine at a final concentration of 0.5μM. Bacteria
644 without brevicidine treatment were used as untreated control. Three replicates were
645 performed for both brevicidine treated and untreated bacterial cultures, 4ml for each
646 sample. After incubation at 37˚C with aeration at 220rpm for 1h, the bacteria from
647 different treatments were collected by centrifuging, and the bacterial pallets were
648 stored in liquid nitrogen immediately. Subsequently, the samples were sent to
649 Novogene Co., Ltd (China) for transcriptome analysis. After RNA extraction, mRNA
650 purification, and cDNA synthesis, the samples were sequenced on the Illumina
651 NovaSeq6000. The quality of the resulting fastq reads was mapped on the reference
652 genome using Bowtie2 2.3.4.3 using default settings. Feature Counts 1.5.0-p3 was
653 used to get the gene counts. DESeq2 1.20 was used to identify all genes, and padj

654 ≤0.05 and |log2 (foldchange) | ≥ 0 of genes between two treatments were regarded
655 as differentially expressed genes (DEGs). The volcano map and KEGG enrichment of
656 DEGs were performed with Magic Novogene package (https://magic.novogene.com).
657 The RNA-Seq data have been deposited in the NCBI Gene Expression Omnibus with
658 the accession number PRJNA872022.

659 Mouse peritonitis–sepsis model

660 Brevicidine was tested against *E. coli* O101 in a mouse peritonitis–sepsis model to
661 assess its *in vivo* bioavailability. BALB/c male mice (n=6 per group) were infected with
662 0.4ml of bacterial suspension (2×10^9 c.f.u. per mouse) via intraperitoneal injection, a
663 concentration that achieves approximately 80% mortality within 48 h post-infection.
664 At 1h post-infection, mice were treated with 0.9% NaCl, brevicidine (40mg/kg),
665 brevicidine (20mg/kg), brevicidine (10mg/kg), or colistin (20mg/kg) via
666 intraperitoneal injection. Mice without *E. coli* O101 infections were used as the
667 normal group control. Once the infected mice died, different organs, including the
668 heart, liver, spleen, lung, and kidney, were collected and homogenized in sterilized
669 PBS for bacterial load quantification. At 24h post-infection, the organs of the survived
670 mice were collected to measure the bacterial load. In addition, the same mouse
671 peritonitis–sepsis model was determined for 7d (n=10), and the bacterial load in the
672 organs of surviving mice was quantified at 7 days post-infection.

673 Statistical analysis

674 GraphPad Prism 8.0 was used to fit the data of Fig 2, Fig 3, Fig 5, Fig 8, S1 Fig, S2 Fig,
675 and S3 Fig. The statistical significance of the data was assessed using a two-tailed
676 Student's t-test with GraphPad Prism 8.0. Correlation analyses were evaluated by

677 Pearson r2, ns: p>0.05, *p<0.05, **p<0.01, ***p<0.001, and ****p<0.0001.

678 Supporting information

679 **S1 Fig. Brevicidine show exceptional low hemolytic activity.** Mice (**A**) and rat (**B**)
680 erythrocytes were incubated with brevicidines at concentrations ranging from 2 to
681 128 μM. Their hemolytic activity was assessed by the release of hemoglobin. Cells
682 treated without a tested compound were used as no-lysis control. Cells treated with
683 10% Triton X-100 were used as complete lysis control. The data are representative of
684 three independent experiments.

685 **S2 Fig. Brevicidine show exceptional low cytotoxicity.** Cytotoxicity of brevicidine
686 against PK-15 cells. The data are representative of three independent experiments.

687 **S3 Fig. Brevicidine significantly reduced the bacterial load of organs of the**
688 **peritonitis-sepsis mouse.** At 7 days post-infection, the survived mice (n = 2 to 6) were
689 euthanized by cervical dislocation. Bacterial loads (Log10 CFU per gram of *E. coli*
690 O101) of the heart (**A**), liver (**B**), spleen (**C**), lung (**D**) and kidney (**E**) were counted. All
691 data were presented as means ± SD (n = 6, or n=2 for the untreated group).
692 Correlation analyses were evaluated by Pearson r2, ns: p > 0.05, *p < 0.05, **p < 0.01,
693 and ***p < 0.001 vs. untreated group.

694 **S4 Fig.** MALDI-TOF MS data of HPLC purified brevicidine.

695 **S1 Table** Strains used in this study.

696

697 **Data Availability Statement:** The transcriptome (RNA sequencing) data that support
698 the findings of this study have been deposited in the NCBI Sequence Read Archive
699 (SRA) with the accession code PRJNA872022.

700 **Finding:** Xinghong Zhao was supported by the Science and Technology Project of
701 Sichuan Province (2022YFH0057). Hongping Wan was supported by the Science and
702 Technology Project of Sichuan Province (2022YFH0062).

703 **Competing Interests:** The authors have declared that no competing interests exist.

704 Acknowledgments

705 We thank Prof. Kui Zhu (National Center for Veterinary Drug Safety Evaluation,
706 College of Veterinary Medicine, China Agricultural University, Beijing, China.) for
707 providing the multidrug resistant *Escherichia coli* (B2 and 16QD) strains.
708

References

1. O'neill JIM. Antimicrobial resistance: tackling a crisis for the health and wealth of nations. Rev Antimicrob Resist. 2014;1: 1–16.
2. Kwon JH, Powderly WG. The post-antibiotic era is here. Science. American Association for the Advancement of Science; 2021. p. 471.
3. Knight GM, Glover RE, McQuaid CF, Olaru ID, Gallandat K, Leclerc QJ, et al. Antimicrobial resistance and COVID-19: Intersections and implications. Elife. 2021;10: e64139.
4. Strathdee SA, Davies SC, Marcelin JR. Confronting antimicrobial resistance beyond the COVID-19 pandemic and the 2020 US election. Lancet. 2020;396: 1050–1053.
5. Lai C-C, Chen S-Y, Ko W-C, Hsueh P-R. Increased antimicrobial resistance during the COVID-19 pandemic. Int J Antimicrob Agents. 2021;57: 106324.
6. Rizvi SG, Ahammad SZ. COVID-19 and antimicrobial resistance: A cross-study. Sci Total Environ. 2022;807: 150873.
7. Butler MS, Blaskovich MAT, Cooper MA. Antibiotics in the clinical pipeline at the end of 2015. J Antibiot (Tokyo). 2017;70: 3.
8. Butler MS, Blaskovich MA, Cooper MA. Antibiotics in the clinical pipeline in 2013. J Antibiot (Tokyo). 2013;66: 571.
9. Roemer T, Boone C. Systems-level antimicrobial drug and drug synergy discovery. Nat Chem Biol. 2013;9: 222.
10. Süssmuth RD, Mainz A. Nonribosomal peptide synthesis—principles and prospects. Angew Chemie Int Ed. 2017;56: 3770–3821.
11. Li Y-X, Zhong Z, Zhang W-P, Qian P-Y. Discovery of cationic nonribosomal peptides as Gram-negative antibiotics through global genome mining. Nat Commun. 2018;9: 3273.
12. Zhao X, Li Z, Kuipers OP. Mimicry of a Non-ribosomally Produced Antimicrobial, Brevicidine, by Ribosomal Synthesis and Post-translational Modification. Cell Chem Biol. 2020;27: 1262-1271.e4. doi:10.1016/j.chembiol.2020.07.005
13. Tacconelli E, Magrini N, Kahlmeter G, Singh N. Global priority list of antibiotic-resistant bacteria to guide research, discovery, and development of new antibiotics. World Heal Organ. 2017;27: 318–327.
14. Song M, Liu Y, Huang X, Ding S, Wang Y, Shen J, et al. A broad-spectrum antibiotic adjuvant reverses multidrug-resistant Gram-negative pathogens. Nat Microbiol. 2020;5: 1040–1050.
15. Liu Y, Shi L, Su L, van der Mei HC, Jutte PC, Ren Y, et al. Nanotechnology-based antimicrobials and delivery systems for biofilm-infection control. Chem Soc Rev. 2019;48: 428–446.
16. Sharma G, Sharma S, Sharma P, Chandola D, Dang S, Gupta S, et al. Escherichia coli biofilm: development and therapeutic strategies. J Appl Microbiol. 2016;121: 309–319.
17. Haney EF, Trimble MJ, Hancock REW. Microtiter plate assays to assess antibiofilm activity against bacteria. Nat Protoc. 2021;16: 2615–2632.

752 18. Zhao X, Yin Z, Breukink E, Moll GN, Kuipers OP. An Engineered Double Lipid II
753 Binding Motifs-Containing Activity against Enterococcus faecium. Antimicrob
754 Agents Chemother. 2020;64: 1–12.
755 19. Ling LL, Schneider T, Peoples AJ, Spoering AL, Engels I, Conlon BP, et al. A new
756 antibiotic kills pathogens without detectable resistance. Nature. 2015;517:
757 455.
758 20. Helander IM, Mattila-Sandholm T. Fluorometric assessment of Gram-negative
759 bacterial permeabilization. J Appl Microbiol. 2000;88: 213–219.
760 21. Cochrane SA, Findlay B, Bakhtiary A, Acedo JZ, Rodriguez-Lopez EM, Mercier P,
761 et al. Antimicrobial lipopeptide tridecaptin A1 selectively binds to
762 Gram-negative lipid II. Proc Natl Acad Sci. 2016;113: 11561–11566.
763 22. Stokes JM, Yang K, Swanson K, Jin W, Cubillos-Ruiz A, Donghia NM, et al. A
764 deep learning approach to antibiotic discovery. Cell. 2020;180: 688–702.
765 23. Wu M, Maier E, Benz R, Hancock REW. Mechanism of interaction of different
766 classes of cationic antimicrobial peptides with planar bilayers and with the
767 cytoplasmic membrane of Escherichia coli. Biochemistry. 1999;38: 7235–7242.
768 24. Ahmed S, Booth IR. The use of valinomycin, nigericin and trichlorocarbanilide
769 in control of the protonmotive force in Escherichia coli cells. Biochem J.
770 1983;212: 105–112.
771 25. Bakker EP, Mangerich WE. Interconversion of components of the bacterial
772 proton motive force by electrogenic potassium transport. J Bacteriol.
773 1981;147: 820–826.
774 26. Winartasaputra H, Mallet VN, Kuan SS, Guilbault GG. Fluorometric and
775 colorimetric enzymic determination of triglycerides (triacylglycerols) in serum.
776 Clin Chem. 1980;26: 613–617.
777 27. McMillian MK, Li L, Parker JB, Patel L, Zhong Z, Gunnett JW, et al. An improved
778 resazurin-based cytotoxicity assay for hepatic cells. Cell Biol Toxicol. 2002;18:
779 157–173.
780 28. Barnes S, Spenney JG. Stoichiometry of the NADH-oxidoreductase reaction for
781 dehydrogenase determinations. Clin Chim acta. 1980;107: 149–154.
782 29. Li Z, Chakraborty P, de Vries RH, Song C, Zhao X, Roelfes G, et al.
783 Characterization of two relacidines belonging to a novel class of circular
784 lipopeptides that act against Gram-negative bacterial pathogens. Environ
785 Microbiol. 2020;22: 5125–5136.
786 30. Sohlenkamp C, Geiger O. Bacterial membrane lipids: diversity in structures
787 and pathways. FEMS Microbiol Rev. 2016;40: 133–159.
788 31. Santos RS, Figueiredo C, Azevedo NF, Braeckmans K, De Smedt SC.
789 Nanomaterials and molecular transporters to overcome the bacterial
790 envelope barrier: Towards advanced delivery of antibiotics. Adv Drug Deliv
791 Rev. 2018;136: 28–48.
792 32. Wiegand I, Hilpert K, Hancock REW. Agar and broth dilution methods to
793 determine the minimal inhibitory concentration (MIC) of antimicrobial
794 substances. Nat Protoc. 2008;3: 163.
795 33. Zhao X, Cui Q, Fu Q, Song X, Jia R, Yang Y, et al. Antiviral properties of

796 resveratrol against pseudorabies virus are associated with the inhibition of IκB
797 kinase activation. Sci Rep. 2017;7. doi:10.1038/s41598-017-09365-0
798 34. Ce R, Silva RC, Trentin DS, Marchi JGB De, Paese K, Guterres SS, et al. Galleria
799 mellonella larvae as an in vivo model to evaluate the toxicity of polymeric
800 nanocapsules. J Nanosci Nanotechnol. 2020;20: 1486–1494.
801 35. Cebrián R, Belmonte-Reche E, Pirota V, de Jong A, Morales JC, Freccero M, et
802 al. G-quadruplex DNA as a target in pathogenic bacteria: efficacy of an
803 extended naphthalene diimide ligand and its mode of action. J Med Chem.
804 2021;65: 4752–4766.
805 36. Li Z, de Vries RH, Chakraborty P, Song C, Zhao X, Scheffers D-J, et al. Novel
806 modifications of nonribosomal peptides from Brevibacillus laterosporus MG64
807 and investigation of their mode of action. Appl Environ Microbiol. 2020;86.
808
809